Metallization of Branched DNA Origami for Nanoelectronic Circuit Fabrication

Jianfei Liu,[†] Yanli Geng,[‡] Elisabeth Pound,[‡] Shailendra Gyawali,[†] Jeffrey R. Ashton,[‡] John Hickey,[†] Adam T. Woolley,[‡] and John N. Harb[†,*]

[†]Department of Chemical Engineering and [‡]Department of Chemistry and Biochemistry, Brigham Young University, Provo, Utah 84602, United States

ABSTRACT This work examines the metallization of folded DNA, known as DNA origami, as an enabling step toward the use of such DNA as templates for nanoelectronic circuits. DNA origami, a simple and robust method for creating a wide variety of shapes and patterns, makes possible the increased complexity and flexibility needed for both the design and assembly of useful circuit templates. In addition, selective metallization of the DNA template is essential for circuit fabrication. Metallization of DNA origami presents several challenges over and above those associated with the metallization of other DNA templates such as λ-DNA. These challenges include (1) the stability of the origami in the processes used for metallization, (2) the enhanced selectivity required to metallize small origami structures, (3) the increased difficulty of adhering small structures to the surface so that they will not be removed when subject to multiple metallization steps, and (4) the influence of excess staple strands present with the origami. This paper describes our efforts to understand and address these challenges. Specifically, the influence of experimental conditions on template stability and on the selectivity of metal deposition was investigated for small DNA origami templates. These templates were seeded with Ag and then plated with Au *via* an electroless deposition process. Both staple strand concentration and the concentration of ions in solution were found to have a significant impact. Selective continuous metal deposition was achieved, with an average metallized height as small as 32 nm. The shape of branched origami was also retained after metallization. These results represent important progress toward the realization of DNA-templated nanocircuits.

KEYWORDS: DNA metallization · DNA origami · electroless deposition · nanoelectronic circuits · nanowire · Au

Integrated circuits have achieved remarkable increases in speed and density over the last two decades. In spite of this, the desire for such increases remains unsatisfied. While current fabrication methods appear adequate to meet demands in the near term, a transformative method that overcomes the limitations inherent in today's semiconductor fabrication methods would aid in meeting long-term needs. Bottom-up nanotechnology, which utilizes the recognition properties of molecules to self-assemble and form nanostructures,[1] provides an alternative fabrication path for future generation nanoelectronic circuits.

Use of DNA as a transistor template was demonstrated by Keren *et al.*, who used λ-DNA and carbon nanotubes to create DNA-templated transistors.[2] While their pioneering work demonstrates proof-of concept, it is not scalable to the complex architectures needed for future generations of devices. DNA origami has been demonstrated as a robust and simple method for creating arbitrary 2-D shapes[3] and different 3-D structures,[4] offering a route to make templates that provide the increased complexity needed for nanoelectronic circuits. Recently, we demonstrated the use of scaffolds of designed lengths prepared by PCR amplification to make branched DNA origami with thin, wire-like structures well-suited for circuit templates.[5] Placement and orientation of DNA origami on a lithographically patterned surface has also recently been demonstrated.[6−8]

One way to form the conductive elements needed for nanocircuits is by metallization of a DNA template. Metallization of DNA to form Ag,[9−13] Au,[14−19] Pd,[20−25] Pt,[26−28] Cu,[29] Ni,[30,31] and Co[32] nanowires has been reported in the literature. Most of these studies have been performed with λ-DNA as it is linear, readily available, and easy to locate on a surface because of its substantial length. A few other types of DNA templates have also been used for metallization including calf thymus DNA,[18] artificially synthesized DNA,[33] DNA nanoribbons,[10] DNA nanotubes,[11,23] and linear three-helix bundles.[12] As selective metallization depends strongly on interactions with the DNA template, specific properties of the template affect the metallization process and an understanding of these interactions is important.[34]

Here we address the metallization of DNA origami, which presents several challenges relative to other DNA templates such as λ-DNA. First, DNA origami tends to be less stable than double-stranded λ-DNA, as it is held together by many short staple strands

*Address correspondence to john_harb@byu.edu.

Received for review December 17, 2010 and accepted February 1, 2011.

Published online February 16, 2011
10.1021/nn1035075

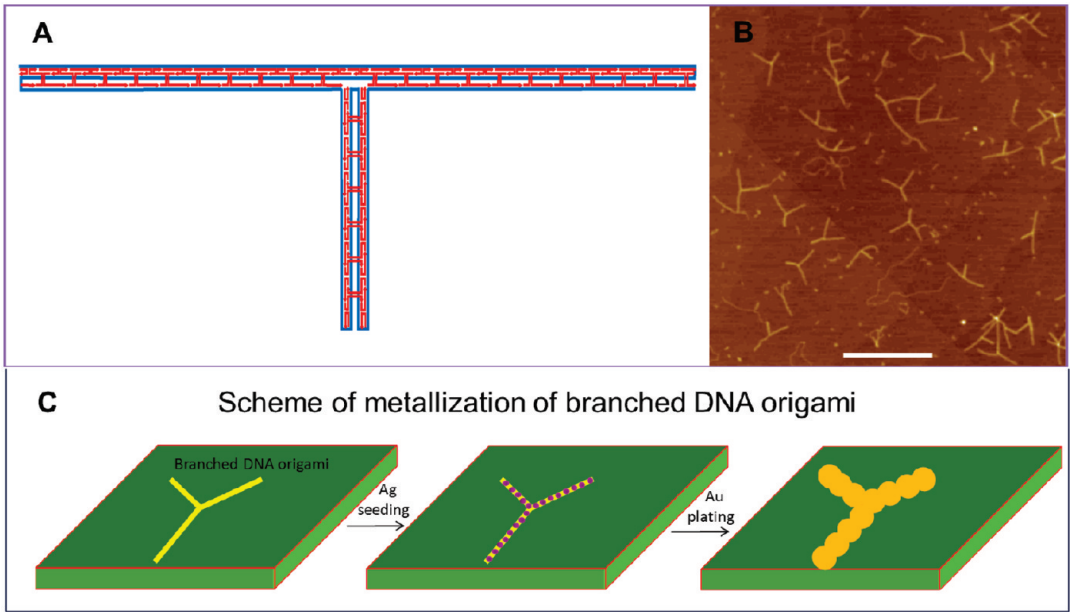

Figure 1. (A) Design of branched origami. (B) Branched origami deposited on mica surface. Scale bar: 500 nm. Height scale: 4 nm. (C) Schematic illustration of DNA origami metallization.

and may unfold. The metallization of DNA usually requires several steps that involve different solutions, concentrations, and/or temperatures; therefore, the DNA template must be sufficiently robust to maintain its shape when subjected to the conditions required for metallization. Second, the small size of the DNA origami makes surface adhesion more difficult due, for example, to fewer attachment points, and requires a higher degree of selectivity to enable identification on the surface after metallization. The small size also requires a high seed density and increased plating precision in order to yield continuous metallization of the DNA origami while preserving its shape. Third, a large excess of staple strands present in the DNA origami assembly solution, while increasing stability, can also impact the selectivity of DNA origami metallization. This paper describes our efforts to understand and address these challenges.

The branched DNA origami used in the current study is shown in Figure 1. We prepared the single-stranded scaffold and folded this branched DNA origami as previously reported using 95 different types of staple strands.[5] DNA origami was folded with both a 10:1 and a 100:1 molar ratio of staple strands to scaffold strands in either TAE-Mg^{2+} buffer (pH = 8.5, 40 mM Tris-Base, 20 mM acetic acid, 1 mM EDTA, 12.5 mM $MgAc_2$) or Hepes-Mg^{2+} buffer (pH = 7.4, 25 mM Hepes, 12.5 mM $MgAc_2$). This branched DNA origami is designed as an asymmetric structure with a 240 nm long top arm and a 75 nm long stem (Figure 1A). The top arm and stem are 3 helices (~8 nm) and 4 helices (~11 nm) wide, respectively. Due to the flexibility in the top arm and the junction, this branched origami resembles a "T" or "Y" when deposited on mica surfaces (Figure 1B). All AFM images in this paper were taken in air with tapping mode AFM. The average height of the non-treated DNA origami on mica surfaces is about 0.6−1.1 nm. A schematic illustration of the metallization of branched DNA origami is shown in Figure 1C.

RESULTS AND DISCUSSION

A primary objective of work described in this paper was to metallize branched DNA origami with little or no background metallization on the surface. In the results that follow, seeding was performed by reacting silver ions with aldehyde groups on chemically modified DNA origami in solution using a procedure modified from that described in refs 10−13. Briefly, DNA origami was cross-linked with amine-modified psoralen and then purified by dialysis. The DNA origami was then functionalized by reacting with glutaraldehyde, followed by another dialysis step to remove excess glutaraldehyde. Afterward, DNA origami was seeded in solution with silver. Electroless plating of gold was subsequently performed on the silver seeds (see Materials and Methods for details).

Retaining the structure of DNA origami during the metallization processes is of key importance for nanocircuit fabrication. There are several aspects of the seeding and plating processes that have the potential to impact the stability of the DNA origami. For the metallization method used in this paper, two of the most important variables are the composition of the rinsing solution and the amount of excess staple strands present in the dialysis procedure.

Rinsing is a frequently used step in DNA metallization processes that has the potential to influence DNA shape and stability. Initial experiments to examine the stability of DNA origami showed that even a 5 s rinse in ultrapure water was sufficient to cause substantial

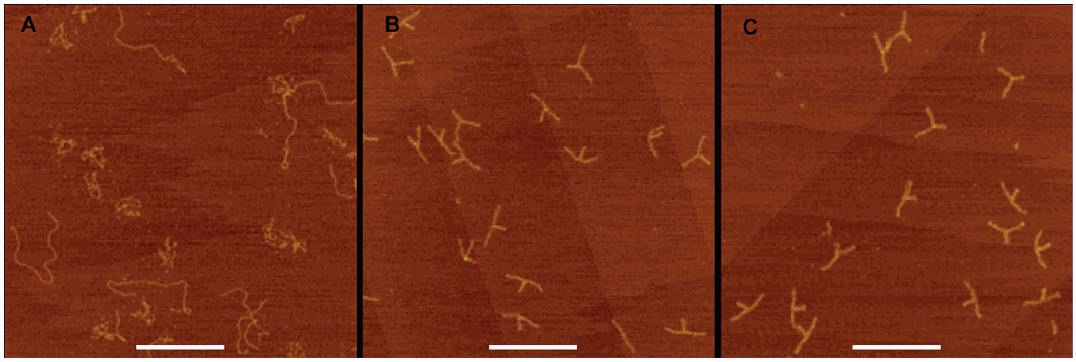

Figure 2. (A) AFM image of branched DNA origami on mica rinsed for 5 s with water. (B) AFM image of branched DNA origami on mica rinsed for 5 s with 4 mM $MgAc_2$. (C) AFM image of branched DNA origami on mica rinsed for 5 s with 4 mM $MgCl_2$. Scale bars: 500 nm. Height scales: 4 nm.

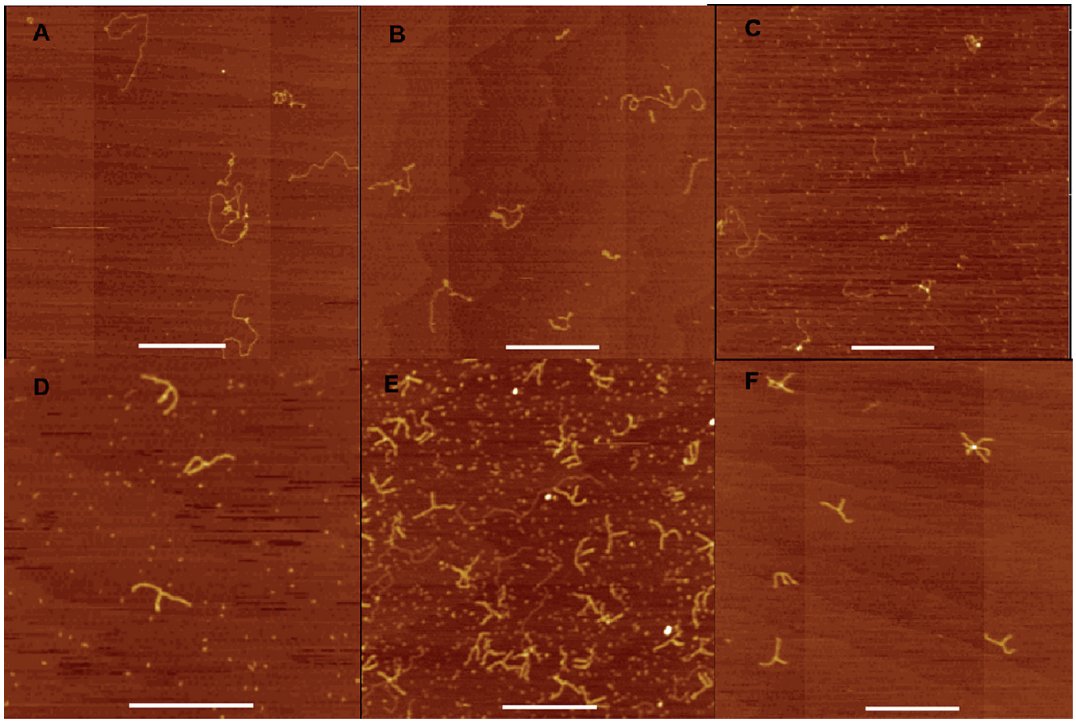

Figure 3. (A−C) AFM images of 2 nM branched DNA origami with a 10:1 molar ratio of staple strands to scaffold after (A) glutaraldehyde reaction and overnight dialysis in water; (B) cross-linking, glutaraldehyde reaction, and overnight dialysis in water; (C) cross-linking, glutaraldehyde reaction, and overnight dialysis in 1× Hepes-Mg^{2+} buffer. (D,E) AFM images of 2 nM branched DNA origami with a 100:1 molar ratio of staple strands to scaffold after cross-linking, glutaraldehyde reaction, and (D) overnight dialysis in water; (E) overnight dialysis in 1× Hepes-Mg^{2+} buffer; (F) 10 nM DNA origami with a 10:1 molar ratio staple strands to scaffold after cross-linking, glutaraldehyde reaction, and overnight dialysis in 1× Hepes-Mg^{2+} buffer. Origami in (D) and (F) was diluted 10 times before deposition on mica surfaces. Scale bars: 500 nm. Height scales: 4 nm.

unfolding of the origami on mica surfaces (Figure 2A) (mica from S&J Trading, Inc., Glen Oaks, NY). However, if the DNA origami was deposited and rinsed (~5 s) with $MgAc_2$ (4 mM) (Figure 2B) or $MgCl_2$ (4 mM) (Figure 2C), it remained folded. Therefore, the presence of magnesium ions increased stability, presumably by reducing the repulsive force between negatively charged scaffold DNA and staple strands.

The seeding and plating processes use solutions of several different compositions, changing the environment to which the DNA origami is exposed and impacting its stability. Perhaps the most aggressive of these steps is the overnight dialysis against a water solution that is used to remove excess glutaraldehyde before seeding the DNA with silver.[2,10−13,16,17] Indeed, we have observed unfolding of the origami during dialysis under several different conditions (Figure 3A). Attempts were made to enhance stability by cross-linking the assembled origami, dialyzing against a buffer solution containing Mg^{2+} (as opposed to just water), adjusting the initial concentration of the origami, and adjusting the staple to scaffold strand ratio.

The DNA origami was cross-linked with an amine-modified psoralen to enhance stability (see Materials and Methods). Initial results seemed to indicate an increase in stability, although the extent of cross-linking was not characterized precisely. The cross-linking also provides additional functional groups (*i.e.*, amine groups) with the potential to increase the seed density by providing sites[35] for metallization. Unfortunately, cross-linking alone did not provide the stability needed for effective dialysis of a 2 nM DNA origami solution with a 10:1 staple to scaffold strand ratio (Figure 3B). However, because of the positive initial results and the fact that the cross-linking did not have a negative impact on our process, we continued to use psoralen cross-linking with our samples.

On the basis of the increased stability observed when rinsing with solutions containing magnesium ions (see above), the stability of the origami was examined for overnight dialysis against a buffer solution containing Mg^{2+}. The results in Figure 3C show that the DNA was not stable and unfolded during dialysis. Therefore, the potential increase in stability due to dialysis in 1× Hepes-Mg^{2+} buffer was not adequate to stabilize the DNA for a 2 nM origami solution with a 10:1 staple to scaffold strand ratio.

Next, the staple to scaffold ratio was increased to 100:1, while the concentration of origami was kept at 2 nM. The hypothesis behind this attempt was that the DNA stability was adversely affected by transfer of staple strands through the membrane during dialysis. Cross-linked DNA was used in order to increase the probability of success, and overnight dialysis was performed against both water (Figure 3D) and 1× Hepes-Mg^{2+} buffer (Figure 3E). The results for both of these dialysis solutions show that the DNA origami retained its structure and remained stable during overnight dialysis when the ratio of staple strands to scaffold strands was increased by a factor of 10. However, this 100:1 molar ratio of staple strands to scaffold has an adverse effect on the selectivity of metallization as discussed in detail later.

An additional experiment was performed in which the ratio of staple to scaffold strands was kept at 10:1, but the concentration of the DNA origami was increased to 10 nM. This more concentrated solution was then dialyzed overnight against a 1× Hepes-Mg^{2+} buffer. Following dialysis, the solution was diluted by a factor of 10 and then deposited on the surface. The results show that the DNA did not unfold during dialysis and that the background concentration of staple strands was greatly reduced (Figure 3F). It also follows that the stability of the origami does not scale linearly with the staple strand to scaffold strand ratio but is influenced by the absolute concentration of staple strands in solution. Also note that the quantity of DNA origami on the surface imaged by AFM was related to not only the concentration of DNA origami in the solution but also the time allowed for surface deposition and rinsing.

From these results, silver seeding in solution was done using cross-linked branched origami dialyzed against 1× Hepes-Mg^{2+} buffer with both a 100:1 and a 10:1 molar ratio of staple strands to scaffold. Figure 4A,B shows branched DNA origami (2 nM origami with 200 nM staple strands) deposited on a mica surface after seeding with silver in solution. Magnesium addition ($MgAc_2$, 10 mM) to the seeded DNA origami solution was used to promote adhesion of the seeded origami to the mica surface, followed by a moderate rinse by dipping into water to remove the seeding solution from the mica surface prior to plating. This moderate rinse step did not decompose or unfold the seeded DNA origami. The extent of seeding is difficult to determine from these images. The primary indication of seeding was an increase in height to 1.5 to 2.0 nm. The origami structures largely retained their shape, and the entire structures appeared to be seeded, although the seeding was not completely uniform as indicated by a variation in height along the structures. Seeding of the background area is also evident in the images. The background deposition is believed to be due to excess staple strands on the surface as no such deposition was observed in the absence of DNA (Figure 4C). The observation that no significant plating was observed for samples that did not go through the seeding process provides strong evidence for both the need for and success of the seeding process.

With an increased understanding of how steps in the seeding processes influence the stability of DNA origami, we will now examine the plating process. Two types of control experiments were performed as a basis for evaluating metallization. First, the entire seeding (including the cross-linking and glutaraldehyde reaction steps) and plating procedures were performed with solutions that did not contain DNA. The expectation was that no plating would occur without the DNA template. The results shown in Figure 5A indicate little or no plating on a mica surface when there was no DNA present. The second control experiment was to deposit unseeded DNA on the surface and then subject it to the gold plating solution. No plating was observed on the unseeded DNA, as evidenced by the lack of significant change in the height of the structures on the surface, even after long plating times (Figure 5B,C). These experiments establish the necessity of having seeded DNA templates on the surface for significant plating to occur.

Initial attempts to plate the seeded origami failed to show any DNA origami (plated or not plated) on the surface during AFM examination. Investigation showed that the problem was actually adhesion of the origami to the surface in the plating solution. The adhesion problem was solved by adding $MgCl_2$ to the electroless Au plating solution to yield a final Mg^{2+} concentration of 2 mM.

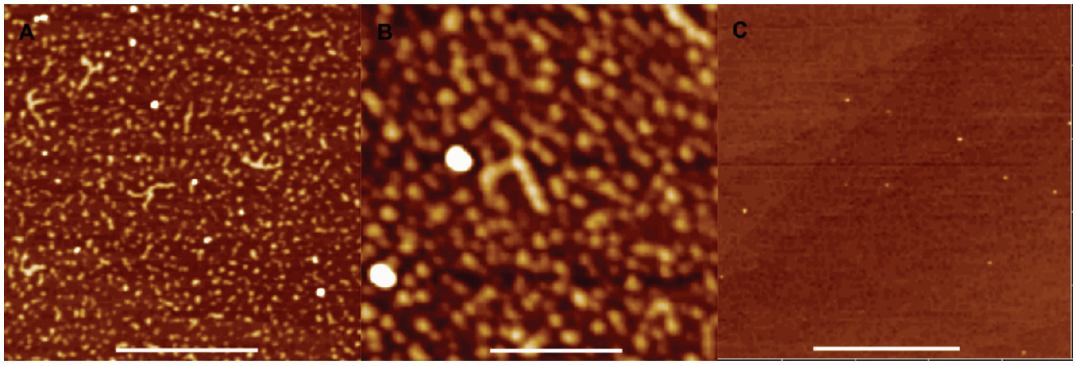

Figure 4. (A,B) AFM images of Ag seeded branched DNA origami, 2 nM scaffold with 100-fold excess staple strands. (C) AFM image of seeding on a control without DNA. Height scales: 4 nm. Scale bar in (A) and (C): 500 nm. Scale bar in (B): 250 nm.

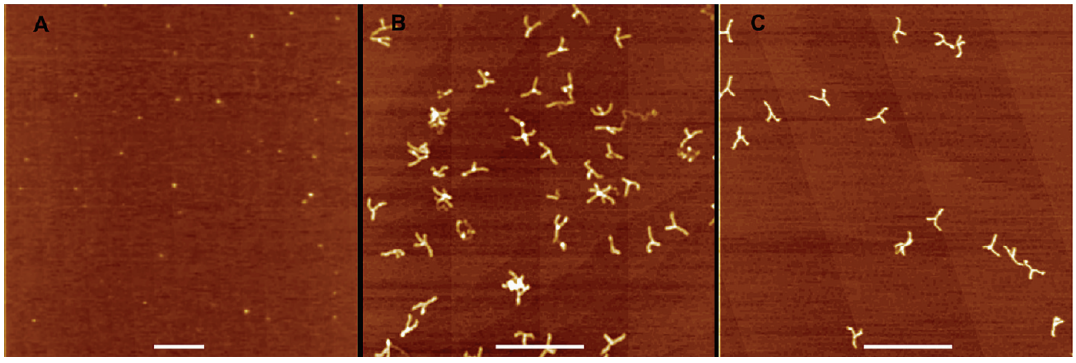

Figure 5. (A) AFM image after 3 min of exposure to the Au plating solution on a control surface without DNA. Height scale: 10 nm. AFM images of nonseeded origami after (B) 5 min and (C) 20 min of immersion in the Au electroless plating bath. Height scales: 4 nm. Scale bars: 500 nm.

Figure 6A shows an AFM image of a branched DNA origami that has been metallized with gold. The starting DNA origami concentration was 2 nM with 100-fold staple strands. It was seeded and then plated with Au for 3 min to yield an average final height of 32 nm. The metallization appears to be continuous, and the selectivity was sufficient to permit distinction of the metallized origami from the background. A lower magnification AFM image provides a surface view with multiple metallized origami, as well as background deposition (Figure 6B). The background deposition was attributed to seeded staple strands and some origami artifacts (*i.e.*, two branches of origami stacked together, or tangled origami) as observed previously above (see Figure 3E).

To get better selectivity, the more concentrated DNA origami described above (10 nM, 10:1 staple to scaffold strand ratio) was used for metallization. Also, a smaller volume of DNA origami solution (10 μL, instead of 25 μL) was used in the seeding process, and the seeded sample was rinsed by dipping in water for 5 s, rather than 2 s, after the origami was deposited onto the surface. The longer rinse after seeding removed a substantial fraction of the staple strands from the surface, as well as some of the seeded origami. After subsequent electroless Au plating for 5 min, origami was seen plated with good selectivity (Figure 6C). The average height of the 5 min plated origami was about 60 nm, which is significantly taller than the sample plated for 3 min (32 nm).

Scanning electron microscopy was also used to examine the morphology and continuity of the metallized, branched DNA origami. SEM images were taken in low-vacuum mode to avoid charging problems on the insulating mica substrate. These images (*e.g.*, Figure 6D,E) provide evidence for continuous metallization. An EDX spectrum (Figure 6F) collected from the plated sample in Figure 6D confirms the presence of Au metal on the origami.

Additional experiments were performed to verify the role of staple strands during metallization because they appear to represent the primary source for the background (nonselective) deposition. Figure 7 shows the results after both seeding (A) and plating (B,C) where the only DNA present was the staple strands (*i.e.*, no origami). Substantial metallization was observed, consistent with the nonselective "background" plating observed in the experiments containing the DNA origami (see Figure 6A,B). It is interesting to note that the number of metal sites after plating was actually less than that observed immediately after the seeding process and was a function of the Mg^{2+} concentration used in the plating solution. The decreased deposition at lower magnesium concentrations is attributed to the

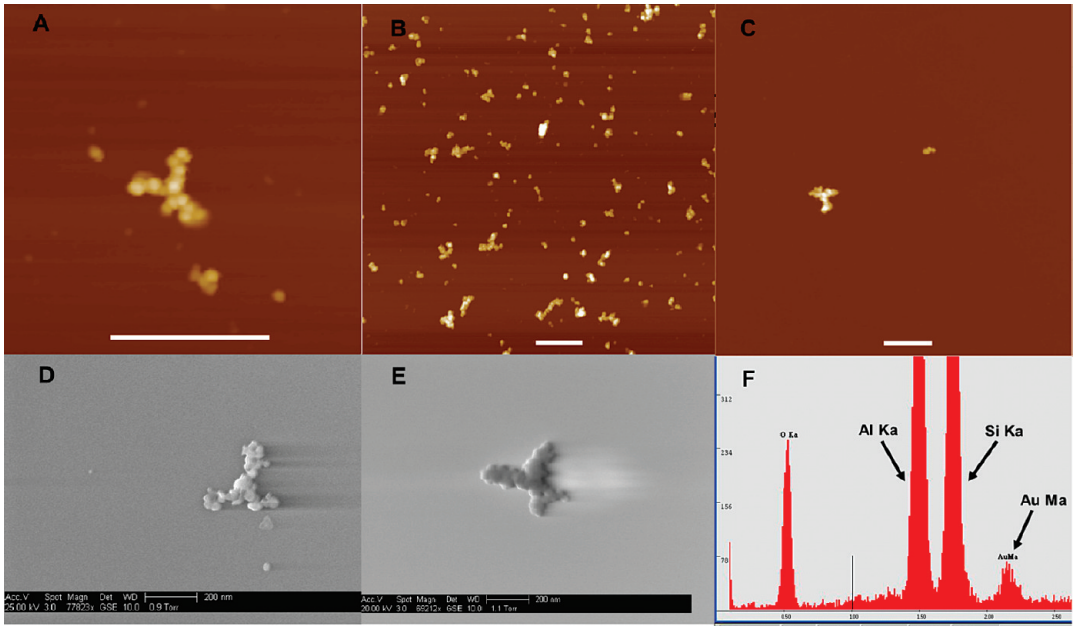

Figure 6. (A,B) AFM images of 2 nM branched origami with a 100:1 molar ratio of staple strands to scaffold after Ag seeding and 3 min of Au plating. (C) AFM image of 10 nM branched origami with a 10:1 molar ratio of staple strands to scaffold after Ag seeding and 5 min of Au plating. (D) SEM image of 2 nM branched origami with a 100:1 molar ratio of staple strands to scaffold after Ag seeding and 3 min of Au plating. (E) SEM image of 10 nM branched origami with a 10:1 molar ratio of staple strands to scaffold after Ag seeding and 5 min of Au plating. SEM images were taken in low-vacuum mode. (F) EDX of the plated origami in image (D). Scale bars in (A−C): 500 nm. Height scales in (A,B): 120 nm. Height scale in (C): 150 nm.

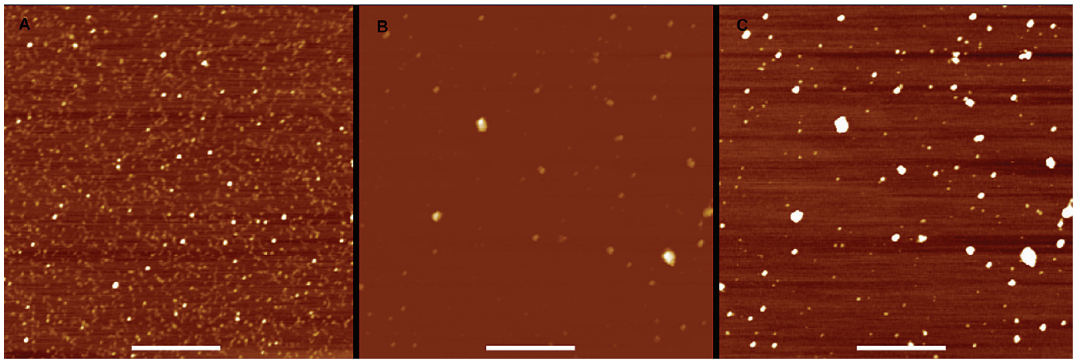

Figure 7. (A) Seeded staple strands (200 nM of each staple strand, equivalent to a 100:1 staple to scaffold strand ratio) on a mica surface. Height scale: 6 nm. (B,C) Seeded, then 3 min of Au plating on staple strands; (B,C) are from AFM images of the same place with different height scales. Height scale in (B): 80 nm. Height scale in (C): 6 nm. Scale bars: 500 nm.

preferential removal of staple strands, which are much smaller than the origami and adhere less strongly to the surface. Therefore, a lower Mg^{2+} concentration (2 mM, lower compared to 10 mM Mg^{2+} for adhering seeded origami to the surface) in the plating solution led to better selectivity for DNA origami metallization, while keeping enough origami on the surface.

Experiments were also performed to examine the stability in the plating solution of DNA origami relative to that of λ-DNA, which is the most frequently used scaffold for DNA metallization. More than 80% of λ-DNA strands deposited on a mica surface were longer than 10 μm (Figure 8A). After incubation in the Au electroless plating solution (with 2 mM $MgCl_2$) for 5 min, 96% of DNA strands found on the surface were shorter than 5 μm long (Figure 8B). Apparently, the plating solution was instrumental in cleaving the λ-DNA. In contrast, the DNA origami maintained its structural integrity in the Au electroless plating solution (with 2 mM $MgCl_2$) over the same period of time (Figure 5B). The structural integrity of the origami is likely due to the presence of multiple helices connected at multiple points through staple strands. Even though some parts of the origami backbone may be cleaved, the principal structure of origami is retained. It was also observed that λ-DNA was not cleaved either in the plating solution (with 2 mM $MgCl_2$) without reducing agent or in only the reducing agent (with 2 mM $MgCl_2$). We observed similar behavior for λ-DNA exposed to an electroless Ni plating solution (20 g/L Na_2SO_4 $6H_2O$, 16 g/L $Na_2C_4H_4O_4$ $6H_2O$, 27 g/L NaH_2PO_2 H_2O, 5 mM $MgSO_4$, pH = 5.0, T = 65 °C). A possibility consistent with these observations is that cleavage was

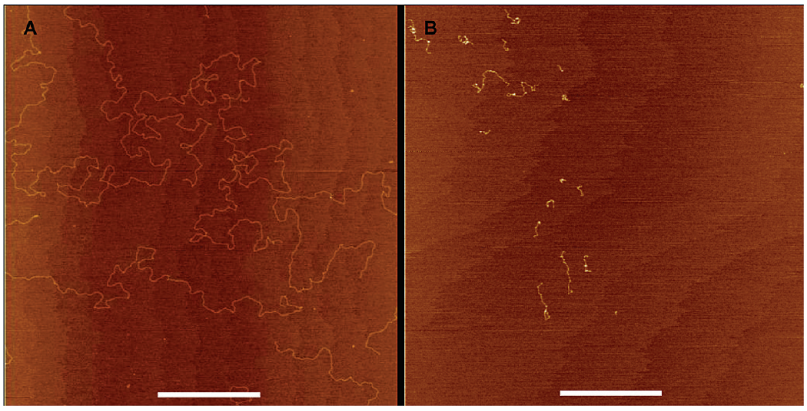

Figure 8. (A) λ-DNA deposited on mica surface. (B) λ-DNA deposited on mica surface, then incubated in Au plating solution for 5 min. Scale bars: 1 μm. Height scales: 4 nm.

caused by a reaction product from the plating reaction. Cleavage of the DNA backbone in an aqueous solution containing complexed metal ions, O_2/H_2O_2, and a reducing agent has been reported in the literature and was attributed to the presence of hydroxyl radicals formed in solution.[36,37]

To conclude, we have demonstrated metallization of branched, open-structured DNA origami with good selectivity. DNA origami has the potential to provide the increasingly complex templates needed for nanocircuit fabrication. However, these structures also present several challenges for metallization as identified and addressed in this study. In particular, challenges associated with the stability of the origami structures during seeding and plating are important. Also, the presence of excess staple strands in solution has a significant impact on selectivity. The successful metallization of branched DNA origami demonstrated here represents important progress toward the realization of DNA-templated nanocircuits. The flexibility of designs possible with DNA origami can also be combined with selective metallization to enable future technologies such as next-generation sensors.[38]

MATERIALS AND METHODS

Materials. Glutaraldehyde and 4′-aminomethyltrioxsalen hydrochloride were purchased from Sigma-Aldrich, Inc.; $AgNO_3$, NH_3H_2O, and the Hepes buffer were obtained from Mallinckrodt Baker. Inc.; $MgCl_2$ and $MgAc_2$ were acquired from EMD Chemical Inc. Slide-A-Lyzer Mini Dialysis units (3500 MWCO) were purchased from Thermo Scientific (Pierce, Rockford, IL). The λ-DNA used in the study was from Worthington Biochemical Corporation. Water used in this research was purified by a Barnstead EASYpure UV/UF system (Barnstead|Thermolyne Corporation) and had a resistivity of 18.3 MΩ·cm.

DNA Origami Cross-Linking. Five milligrams of 4′-aminomethyltrioxsalen hydrochloride was dissolved in 2 mL of ethanol, wrapped with aluminum foil and kept in a refrigerator until use. Then, 100 μL of DNA origami solution (either 2 or 10 nM origami) was mixed with 10 μL of 500 mM NaCl and 10 μL of 4′-aminomethyltrioxsalen hydrochloride and then refrigerated for 15 min. Subsequently, the solution was put on ice in a plastic Petri dish under UV light (λ = 365 nm) for 30 min. To remove excess 4′-aminomethyltrioxsalen hydrochloride, NaCl, and EDTA, the solution was dialyzed against 1× Hepes buffer (25 mM Hepes, 4 mM magnesium acetate, pH = 7.4) for 10 h in a refrigerator using a 3.5k MWCO membrane. The cross-linked and dialyzed DNA origami was then stored in a freezer at −20 °C until use.

DNA Origami Modification and Seeding. Fifty microliters of cross-linked DNA origami solution was diluted to 100 μL with water, followed by the addition of 16 μL of 2.5% glutaraldehyde to react with the DNA origami. The reaction was allowed to take place at room temperature for 30 min. Afterward, the sample was transferred onto ice for 20 min. The excess glutaraldehyde was then removed by dialysis (at least 24 h) using a 3.5k MWCO membrane against ultrapure water or 1× Hepes buffer (25 mM Hepes, 4 mM magnesium acetate, pH = 7.4) in the refrigerator. Subsequently, 25 or 10 μL of reacted DNA origami solution was diluted to 50 μL with water and then mixed with 50 μL of basic silver nitrate solution (0.1 M $AgNO_3$, 0.33 M ammonia hydroxide) in order for seeding to occur. The seeding process was allowed to proceed for 30 min in the dark on ice. Then, $MgAc_2$ was added to increase the Mg^{2+} concentration of the DNA origami solution to 10 mM. Afterward, 4 μL of seeded DNA solution was put on a freshly cleaved mica surface. The adsorption of DNA origami onto the mica surface was allowed to take place for 2 min. Then, the sample was rinsed by dipping in water for 2 or 5 s. After that, the water left on the mica surface was absorbed from the edge by a paper towel, and any remaining moisture was allowed to evaporate.

Electroless Plating. The plating solution was made by mixing equal volumes of 4 mM $MgCl_2$ and a commercial Au plating solution (GoldEnhance EM, Catalog #2113, Nanoprobes, Yaphank, NY). Electroless Au plating solution was put on the surface immediately after the seeding process once the sample became dry. The electroless plating was allowed to proceed for 1−5 min. For the control samples, longer plating times of 10 and 20 min were also explored. Afterward, the sample was rinsed with 4 mM $MgCl_2$ for 5 s and then with water for 2−3 s, followed by drying using a stream of filtered air.

SEM Imaging. Plated origami samples on insulating mica surfaces were imaged in low-vacuum mode on a Philips XL30 ESEM FEG. EDX analysis was also performed on this ESEM by using spot scan.

AFM Imaging. The samples were imaged in air using tapping mode on a Digital Instruments Nanoscope IIIa MultiMode AFM (Veeco) with silicon AFM tips (AppNano FORTA tips from Nanoscience Instruments, Inc.).

Acknowledgment. The authors gratefully acknowledge funding from the National Science Foundation (CBET-0708347). Gratitude is also expressed to Dr. John Gardner, James Havican, Dr. Weichun Yang, and Jayson Pagaduan of BYU for their help and valuable insights.

REFERENCES AND NOTES

1. Seeman, N. C. DNA in a Material World. *Nature* **2003,** *421*, 427–431.
2. Keren, K.; Berman, R. S.; Buchstab, E.; Sivan, U.; Braun, E. DNA-Templated Carbon Nanotube Field-Effect Transistor. *Science* **2003,** *302*, 1380–1382.
3. Rothemund, P. W. K. Folding DNA To Create Nanoscale Shapes and Patterns. *Nature* **2006,** *440*, 297–302.
4. Douglas, S. M.; Dietz, H.; Liedl, T.; Hogberg, B.; Graf, F.; Shih, W. M. Self-Assembly of DNA into Nanoscale Three-Dimensional Shapes. *Nature* **2009,** *459*, 414–418.
5. Pound, E.; Ashton, J. R.; Becerril, H. A.; Woolley, A. T. Polymerase Chain Reaction Based Scaffold Preparation for the Production of Thin, Branched DNA Origami Nanostructures of Arbitrary Sizes. *Nano Lett.* **2009,** *9*, 4302–4305.
6. Ding, B. Q.; Wu, H.; Xu, W.; Zhao, Z. A.; Liu, Y.; Yu, H. B.; Yan, H. Interconnecting Gold Islands with DNA Origami Nanotubes. *Nano Lett.* **2010,** *10*, 5065–5069.
7. Kershner, R. J.; Bozano, L. D.; Micheel, C. M.; Hung, A. M.; Fornof, A. R.; Cha, J. N.; Rettner, C. T.; Bersani, M.; Frommer, J.; Rothemund, P. W. K.; Wallraff, G. M. Placement and Orientation of Individual DNA Shapes on Lithographically Patterned Surfaces. *Nat. Nanotechnol.* **2009,** *4*, 557–561.
8. Hung, A. M.; Micheel, C. M.; Bozano, L. D.; Osterbur, L. W.; Wallraff, G. M.; Cha, J. N. Large-Area Spatially Ordered Arrays of Gold Nanoparticles Directed by Lithographically Confined DNA Origami. *Nat. Nanotechnol.* **2010,** *5*, 121–126.
9. Braun, E.; Eichen, Y.; Sivan, U.; Ben-Yoseph, G. DNA-Templated Assembly and Electrode Attachment of a Conducting Silver Wire. *Nature* **1998,** *391*, 775–778.
10. Yan, H.; Park, S. H.; Finkelstein, G.; Reif, J. H.; LaBean, T. H. DNA-Templated Self-Assembly of Protein Arrays and Highly Conductive Nanowires. *Science* **2003,** *301*, 1882–1884.
11. Liu, D.; Park, S. H.; Reif, J. H.; LaBean, T. H. DNA Nanotubes Self-Assembled from Triple-Crossover Tiles as Templates for Conductive Nanowires. *Proc. Natl. Acad. Sci. U.S.A.* **2004,** *101*, 717–722.
12. Park, S. H.; Barish, R.; Li, H. Y.; Reif, J. H.; Finkelstein, G.; Yan, H.; LaBean, T. H. Three-Helix Bundle DNA Tiles Self-Assemble into 2D Lattice or 1D Templates for Silver Nanowires. *Nano Lett.* **2005,** *5*, 693–696.
13. Park, S. H.; Prior, M. W.; LaBean, T. H.; Finkelstein, G. Optimized Fabrication and Electrical Analysis of Silver Nanowires Templated on DNA Molecules. *Appl. Phys. Lett.* **2006,** *89*, 033901.
14. Aherne, D.; Satti, A.; Fitzmaurice, D. Diameter-Dependent Evolution of Failure Current Density of Highly Conducting DNA-Templated Gold Nanowires. *Nanotechnology* **2007,** *18*, 125205.
15. Harnack, O.; Ford, W. E.; Yasuda, A.; Wessels, J. M. Tris(hydroxymethyl)phosphine-Capped Gold Particles Templated by DNA as Nanowire Precursors. *Nano Lett.* **2002,** *2*, 919–923.
16. Keren, K.; Berman, R. S.; Braun, E. Patterned DNA Metallization by Sequence-Specific Localization of a Reducing Agent. *Nano Lett.* **2004,** *4*, 323–326.
17. Keren, K.; Krueger, M.; Gilad, R.; Ben-Yoseph, G.; Sivan, U.; Braun, E. Sequence-Specific Molecular Lithography on Single DNA Molecules. *Science* **2002,** *297*, 72–75.
18. Ongaro, A.; Griffin, F.; Beeeher, P.; Nagle, L.; Iacopino, D.; Quinn, A.; Redmond, G.; Fitzmaurice, D. DNA-Templated Assembly of Conducting Gold Nanowires between Gold Electrodes on a Silicon Oxide Substrate. *Chem. Mater.* **2005,** *17*, 1959–1964.
19. Kundu, S.; Liang, H. Microwave Synthesis of Electrically Conductive Gold Nanowires on DNA Scaffolds. *Langmuir* **2008,** *24*, 9668–9674.
20. Richter, J.; Mertig, M.; Pompe, W.; Monch, I.; Schackert, H. K. Construction of Highly Conductive Nanowires on a DNA Template. *Appl. Phys. Lett.* **2001,** *78*, 536–538.
21. Richter, J.; Mertig, M.; Pompe, W.; Vinzelberg, H. Low-Temperature Resistance of DNA-Templated Nanowires. *Appl. Phys. A* **2002,** *74*, 725–728.
22. Deng, Z. X.; Mao, C. D. DNA-Templated Fabrication of 1D Parallel and 2D Crossed Metallic Nanowire Arrays. *Nano Lett.* **2003,** *3*, 1545–1548.
23. Liu, H. P.; Chen, Y.; He, Y.; Ribbe, A. E.; Mao, C. D. Approaching the Limit: Can One DNA Oligonucleotide Assemble into Large Nanostructures?. *Angew. Chem., Int. Ed.* **2006,** *45*, 1942–1945.
24. Nguyen, K.; Monteverde, M.; Filoramo, A.; Goux-Capes, L.; Lyonnais, S.; Jegou, P.; Viel, P.; Goffman, M.; Bourgoin, J. P. Synthesis of Thin and Highly Conductive DNA-Based Palladium Nanowires. *Adv. Mater.* **2008,** *20*, 1099–1104.
25. Kundu, S.; Wang, K.; Huitink, D.; Liang, H. Photoinduced Formation of Electrically Conductive Thin Palladium Nanowires on DNA Scaffolds. *Langmuir* **2009,** *25*, 10146–10152.
26. Ford, W. E.; Harnack, O.; Yasuda, A.; Wessels, J. M. Platinated DNA as Precursors to Templated Chains of Metal Nanoparticles. *Adv. Mater.* **2001,** *13*, 1793–1797.
27. Seidel, R.; Ciacchi, L. C.; Weigel, M.; Pompe, W.; Mertig, M. Synthesis of Platinum Cluster Chains on DNA Templates: Conditions for a Template-Controlled Cluster Growth. *J. Phys. Chem. B* **2004,** *108*, 10801–10811.
28. Mertig, M.; Ciacchi, L. C.; Seidel, R.; Pompe, W.; De Vita, A. DNA as a Selective Metallization Template. *Nano Lett.* **2002,** *2*, 841–844.
29. Monson, C. F.; Woolley, A. T. DNA-Templated Construction of Copper Nanowires. *Nano Lett.* **2003,** *3*, 359–363.
30. Becerril, H. A.; Ludtke, P.; Willardson, B. M.; Woolley, A. T. DNA-Templated Nickel Nanostructures and Protein Assemblies. *Langmuir* **2006,** *22*, 10140–10144.
31. Gu, Q.; Cheng, C. D.; Suryanarayanan, S.; Dai, K.; Haynie, D. T. DNA-Templated Fabrication of Nickel Nanocluster Chains. *Physica E* **2006,** *33*, 92–98.
32. Gu, Q.; Haynie, D. T. Palladium Nanoparticle-Controlled Growth of Magnetic Cobalt Nanowires on DNA Templates. *Mater. Lett.* **2008,** *62*, 3047–3050.
33. Fischler, M.; Simon, U.; Nir, H.; Eichen, Y.; Burley, G. A.; Gierlich, J.; Gramlich, P. M. E.; Carell, T. Formation of Bimetallic Ag−Au Nanowires by Metallization of Artificial DNA Duplexes. *Small* **2007,** *3*, 1049–1055.
34. Becerril, H. A.; Woolley, A. T. DNA-Templated Nanofabrication. *Chem. Soc. Rev.* **2009,** *38*, 329–337.
35. Patolsky, F.; Weizmann, Y.; Lioubashevski, O.; Willner, I. Au-Nanoparticle Nanowires Based on DNA and Polylysine Templates. *Angew. Chem., Int. Ed.* **2002,** *41*, 2323–2327.
36. Tullius, T. D.; Dombroski, B. A. Hydroxyl Radical Footprinting—High-Resolution Information about DNA Protein Contacts and Application to Lambda-Repressor and CRO Protein. *Proc. Natl. Acad. Sci. U.S.A.* **1986,** *83*, 5469–5473.
37. Hertzberg, R. P.; Dervan, P. B. Cleavage of DNA with Methidiumpropyl-EDTA-Iron(II)-Reaction Conditions and Product Analyses. *Biochemistry* **1984,** *23*, 3934–3945.
38. Yogeswaran, U.; Chen, S. M. A Review on the Electrochemical Sensors and Biosensors Composed of Nanowires as Sensing Material. *Sensors* **2008,** *8*, 290–313.